

CHALMERS
UNIVERSITY OF TECHNOLOGY

Modeling of Conformal Reflectarrays Through Domain Decomposition Using a Generalized Admittance Approach

Downloaded from: https://research.chalmers.se, 2026-11-24 17:07 UTC

Citation for the original published paper (version of record):
Lin, D., Yadranjee Aghdam, P., Maaskant, R. (2025). Modeling of Conformal Reflectarrays Through Domain Decomposition Using a Generalized Admittance
Approach. Asia-Pacific Microwave Conference Proceedings, APMC.
http://dx.doi.org/10.1109/APMC65046.2025.11378698

N.B. When citing this work, cite the original published paper.

© 2025 IEEE. Personal use of this material is permitted. Permission from IEEE must be obtained for all other uses, in any current or future media, including reprinting/republishing this material for advertising or promotional purposes, or reuse of any copyrighted component of this work in other works.

(article starts on next page)

Modeling of Conformal Reflectarrays Through Domain Decomposition Using a Generalized Admittance Approach

Dijun Lin[#$], Parisa Aghdam[$], Rob Maaskant[#]

[#]Department of Electrical Engineering, Chalmers University of Technology, Gothenburg, Sweden

[$]Ericsson Research, Gothenburg, Sweden

{dijun, Rob.maaskant}@chalmers.se, {dijun.lin, parisa.aghdam}@ericsson.com

***Abstract*— This paper presents a method-of-moments-based domain decomposition technique for analyzing conformal cavity-backed reflectarrays. Scattering from a 3D conformal all-metal reflectarray is modeled using the perfect electric conductor (PEC) equivalence, where impressed aperture magnetic current sources on the cavity apertures separate the interior and exterior cavity domains via a generalized aperture admittance approach. The methodology is evaluated for two representative conformal shapes, concave and convex. Numerical results demonstrate high accuracy, with average relative errors ranging from 0.5% to 2.2%, confirming the validity of the proposed method for finite conformal cavity-backed reflectarrays.**

***Keywords*— Aperture admittance, conformal antennas, domain decomposition, method of moments, radiation pattern, reflectarray antennas.**

I. Introduction

Reconfigurable intelligent surfaces (RIS) have recently attracted significant research interest due to their promising features, such as beamforming and the ability to enhance propagation channels through controlled reflections [1], [2]. Reflectarrays are a notable example of RIS, offering controllable reflections via adjustable phase responses on the array surface. Conventional flat reflectarrays face key limitations, including narrow bandwidth and restricted beam-scanning capability, primarily due to phase errors and element pattern degradation at large off-boresight angles. To address these limitations, conformal arrays are being actively investigated [3]–[6].

Reflectarrays are increasingly considered for applications in satellite communications, aircraft, and UAVs. In these contexts, conformal designs offer advantages, such as enhanced bandwidth and improved side lobe control [7], [8]. However, modeling conformal reflectarrays presents a greater challenge as they are inherently non-periodic. This complexity is further amplified in special cases, such as partially embedded reflectors or SIW-based wideband elements, where the array size and additional features (e.g., via-fencing) significantly increase computational demands [9], [10].

This work builds on our prior research [11], [12] on PEC-equivalent modeling of cavity-backed reflectarray elements in periodic and aperiodic configurations. Here, we illustrate the general setup and modeling methodology for electrically connected *conformal* reflectarrays, demonstrating the effectiveness of the approach using both concave and convex faceted examples.

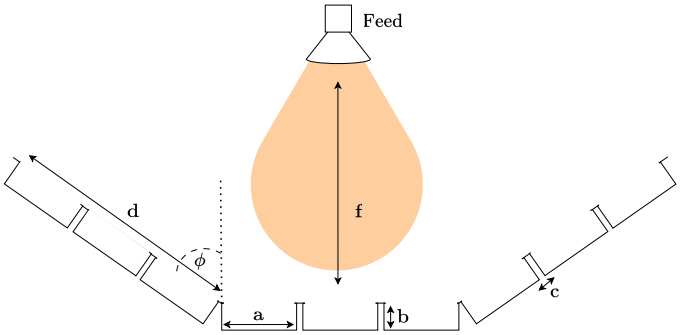

Fig. 1. Baseline configuration: a 3-facet reflectarray illuminated by a center-fed single-pol horn at 1 GHz. Parameters are $a = 0.055$ m, $b = \lambda/2$, $c = \lambda/10$, $d = 1.8\lambda$, $f = 2$ m.

The remainder of this paper is organized as follows. Sec. II details the domain-decomposition-based modeling methodology for conformal arrays. Sec. III presents validation results for both concave and convex faceted reflectarray examples, and Sec. IV concludes the paper and discusses recommendations for future work.

II. Methodology

The modeling methodology used in this work builds on the framework described in [11]. In brief, to model the fields in the exterior region, the metal cavities shown in Fig. 1 are closed with perfect electric conductor (PEC) material. The aperture fields are then represented by equivalent magnetic currents placed on the PEC apertures, as shown in Fig. 2. This procedure is general and can be applied regardless of the unit cell's position or orientation, allowing analysis of both convex and concave reflectarrays.

The over-the-air coupling between aperture field modes (or their equivalent magnetic current representations) is captured by the generalized admittance matrix $\mathbf{Y}^a$, where each entry represents the self- or mutual admittance between a pair of modes. In Fig. 2, $\boldsymbol{M}_n$ denotes the set of K_n equivalent

aperture currents corresponding to the K_n field modes at aperture n, for $n = 1, \ldots, N$.

The coupling among the K_n aperture modes inside the N individual cavities is modeled by the interior admittance matrix, represented as the sparse block-diagonal matrix

$$\mathbf{Y}^b = \begin{bmatrix} \mathbf{Y}_1^b & 0 & \cdots & 0 \\ 0 & \mathbf{Y}_2^b & \cdots & 0 \\ \vdots & \vdots & \ddots & \vdots \\ 0 & 0 & \cdots & \mathbf{Y}_N^b \end{bmatrix} \tag{1}$$

By enforcing field continuity across the apertures, the interior and exterior regions are connected via the admittance formulation [11, Eq. (24)]

$$\left[\mathbf{Y}^a + \mathbf{Y}^b\right] \mathbf{V} = \mathbf{I}, \tag{2}$$

where $\mathbf{V}$ is the vector of aperture field mode amplitudes, and $\mathbf{I}$ is the magnetic excitation vector due to an external feed.

In this decomposition, $\mathbf{Y}^a$ depends on the geometry and positioning of the cells, while $\mathbf{Y}^b$ remains fixed for a given unit cell design. As a result, the method supports flexible array configurations and is well-suited for modeling conformal reflectarrays.

The total magnetic current distribution $\boldsymbol{M}$, as well as each individual mode in the above formulation, radiates in the presence of the surrounding PEC structure. To compute the total scattered field, the PEC surface is replaced by its induced electric surface current $\boldsymbol{J}$. This current is found by solving the electric field integral equation (EFIE):

$$\boldsymbol{E}_{\text{tan}} = \boldsymbol{E}_{\text{tan}}^{\text{i}} + \boldsymbol{E}_{\text{tan}}^{\text{s}}(\boldsymbol{J}) = \mathbf{0}, \tag{3}$$

evaluated at observation points on the PEC surface. Here, $\boldsymbol{E}_{\text{tan}}^{\text{i}} = \boldsymbol{E}_{\text{tan}}(\boldsymbol{M}) + \boldsymbol{E}_{\text{tan}}^{\text{Feed}}$ is the total incident field resulting from the aperture magnetic currents and the feed. The total scattered field in the exterior region thus arises from both the magnetic current $\boldsymbol{M}$ and the induced electric current $\boldsymbol{J}$.

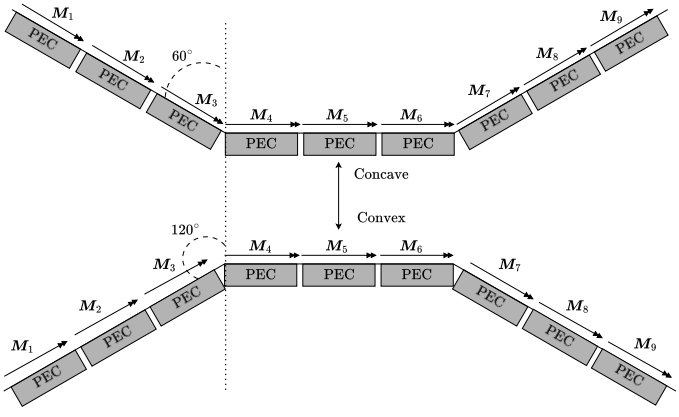

Fig. 2. Exterior PEC-equivalent model for convex and concave reflectarrays.

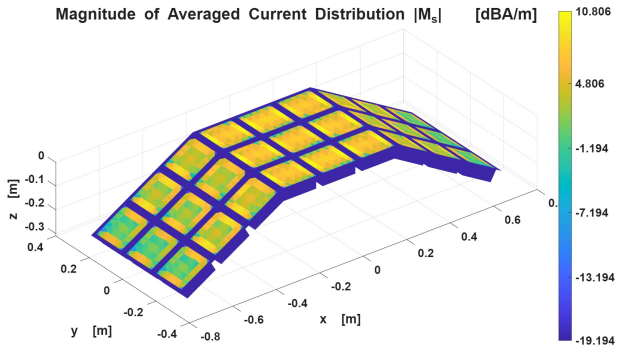

Fig. 3. Equivalent convex array with computed magnetic current distribution

III. Results

The proposed methodology is validated on a 27-element reflectarray in both convex and concave configurations. Each array consists of three 3×3 panels, with the side panels rotated as shown in Fig. 1. In this setup, feed blockage effects are neglected. Both configurations, illustrated in Fig. 2, are selected for their relevance in achieving higher bandwidth and improved wide-angle scanning performance.

Results are compared against a full-wave EFIE-based method-of-moments solver using an identical fixed mesh, enabling direct and consistent benchmarking.

For the convex array, the equivalent magnetic currents are shown in Fig. 3, and the corresponding far-field radiation pattern is plotted in Fig. 4. In the E-plane, the configuration yields an average error of 0.76%, a peak error of 3.91%, and a median of 0.49%. In the H-plane, the average, peak, and median errors are 0.34%, 2.14%, and 0.054%, respectively.

For the concave array (Fig. 5), the radiation pattern is shown in Fig. 6. In the E-plane, the average error is 2.21%, with a peak of 16.43% and a median of 0.90%. In the H-plane, the average, peak, and median errors are 0.53%, 3.57%, and 0.31%, respectively.

We found that the error in the concave array decreases as the mesh density increases, likely due to stronger coupling and more complex current modes that are not adequately captured with the same mesh as the convex array. This trend is also observed between the H- and E-planes, with the latter exhibiting the highest coupling. Overall, these results confirm that the proposed methodology maintains high accuracy across different conformal geometries. Most errors remain below 1% on average, with particularly low median values in both principal planes, demonstrating the robustness of the approach.

IV. Conclusion

This paper validates a domain-decomposition-based generalized admittance matrix approach for the analysis of conformal reflectarrays. High accuracy is demonstrated through comparison with a conventional full-wave method-of-moments solver for a 27-element reflectarray in both convex and concave configurations.

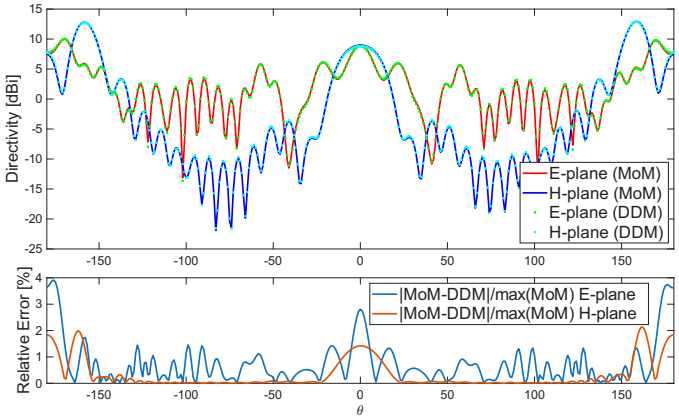

Fig. 4. Radiation pattern and the relative error for the convex array

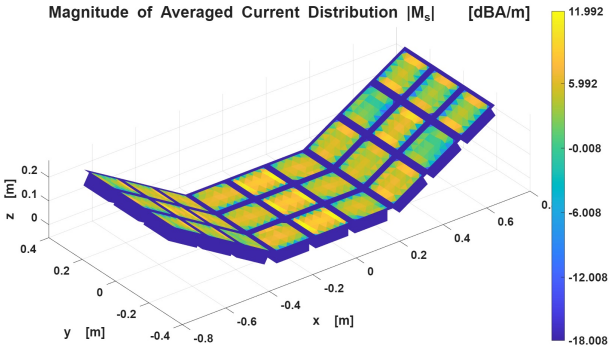

Fig. 5. Equivalent concave array with computed magnetic current distribution

The proposed modular modeling strategy enables efficient reflectarray optimization. For example, in arrays composed of repeated cell types, only partial matrix updates are required to reflect changes in the array lattice. Similarly, when only the cell types are modified, field solutions can be obtained with minimal computational overhead.

Future work will focus on hybridizing this method with high-frequency techniques, such as physical optics, in combination with macro-domain basis functions for current modeling. This hybridization aims to further reduce solution time and memory requirements, enabling efficient simulation of electrically large conformal reflectarrays.

ACKNOWLEDGMENT

This work was funded by the European Union, under ANTERRA 101072363 HORIZON-MSCA-2021-DN-01. Views and opinions expressed are however those of the author(s) only and do not necessarily reflect those of the European Union. Neither the European Union nor the granting authority can be held responsible for them.

REFERENCES

[1] Z. Zhu, C. Pan, Q. Wu, M. D. Renzo, A. L. Swindlehurstand, and Y. Zhao, "Special Issue on Reconfigurable Intelligent Surface for B5G & 6G," Tech. Rep. 5, 2022, p. 513.

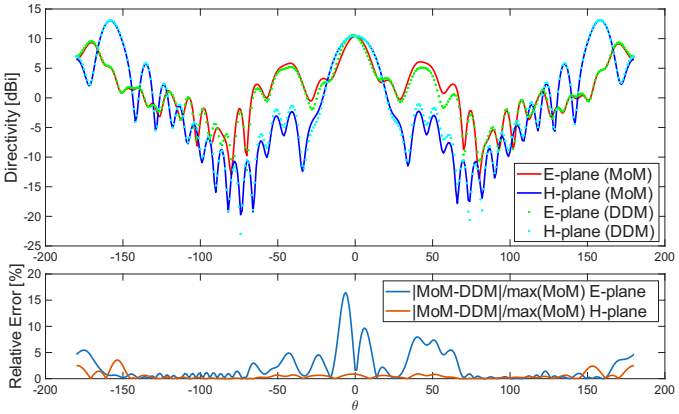

Fig. 6. Radiation pattern and the relative error for the concave array

[2] M. Di Renzo, A. Zappone, M. Debbah, M. S. Alouini, C. Yuen, J. De Rosny, *et al.*, "Smart Radio Environments Empowered by Reconfigurable Intelligent Surfaces: How It Works, State of Research, and the Road Ahead," *IEEE Journal on Selected Areas in Communications*, vol. 38, no. 11, pp. 2450–2525, Nov. 2020.

[3] V. Patel, P. Mevada, D. Pujara, S. Chakrabarty, and M. Mahajan, "Analysis of Multi-Faceted Reflectarray Antenna for Spatial Bandwidth Improvement," in *2020 IEEE International Symposium on Antennas and Propagation and North American Radio Science Meeting, IEEECONF 2020 - Proceedings*, Institute of Electrical and Electronics Engineers Inc., Jul. 2020, pp. 359–360.

[4] B. Imaz-Lueje, M. R. Pino, and M. Arrebola, "Deployable Multi-Faceted Reflectarray Antenna in Offset Configuration With Band Enhancement," *IEEE Transactions on Antennas and Propagation*, vol. 70, no. 12, pp. 11 686–11 696, Dec. 2022.

[5] M. Beccaria, P. Pirinoli, and M. Orefice, "On the bandwidth of convex conformal reflectarray antennas," in *2016 International Workshop on Antenna Technology, iWAT 2016*, Institute of Electrical and Electronics Engineers Inc., Mar. 2016, pp. 92–94.

[6] C. T. Tong, C. En, F. Raelene, and K. C. Tian, "Comparison of Simulated Performance of Faceted & Flat Reflectarray Antennas," in *2018 International Symposium on Antennas and Propagation (ISAP)*, 2018.

[7] M. Zhou, S. B. Sørensen, P. Meincke, and E. Jørgensen, "Design and optimization of multi-faceted reflectarrays for satellite applications," in *8th European Conference on Antennas and Propagation, EuCAP 2014*, Institute of Electrical and Electronics Engineers Inc., 2014, pp. 1423–1427.

[8] D. Martinez-de Rioja, E. Martinez-de Rioja, Y. Rodriguez-Vaqueiro, J. A. Encinar, A. Pino, M. Arias, *et al.*, "Transmit–Receive Parabolic Reflectarray to Generate Two Beams per Feed for Multispot Satellite Antennas in Ka -Band," *IEEE Transactions on Antennas and Propagation*, vol. 69, no. 5, pp. 2673–2685, May 2021.

[9] J. Budhu, S. V. Hum, S. Ellingson, and R. M. Buehrer, "Design of Rim-Located Reconfigurable Reflectarrays for Interference Mitigation in Reflector Antennas," *IEEE Transactions on Antennas and Propagation*, vol. 72, no. 4, pp. 3736–3741, Apr. 2024.

[10] A. Gómez-Álvarez, N. Delmonte, L. Silvestri, M. Bozzi, M. Arrebola, and M. R. Pino, "Dual-Resonance SIW-Based Reflectarray Unit Cell for Broadband Applications," in *2024 18th European Conference on Antennas and Propagation (EuCAP)*, IEEE, Mar. 2024, pp. 1–5.

[11] R. Maaskant, D. Lin, F. Maxharraj, M. Ghaderi Aram, L. Manholm, P. Aghdam, *et al.*, "Domain Decomposition Analysis of Open-cavity-based Array Elements—Roadmap Toward Analyzing Large-Scale Reflectarrays and Reconfigurable Intelligent Surfaces," in *Proceedings of the International Conference on Electromagnetics in Advanced Applications (ICEAA)*, Accepted; to appear, 2025.

[12] D. Lin, L. Manholm, O. Talcoth, S. Agneessens, P. Aghdam, and R. Maaskant, "Fast Scattering Analysis of Large Open-cavity Based Reflectarrays Using a Hybrid Method of Moment and Physical Optics Approach," in *Proceedings of the International Conference on Electromagnetics in Advanced Applications (ICEAA)*, Accepted; to appear, 2025.